Multiphonon-assisted anti-Stokes and Stokes fluorescence of triply ionized rare-earth ions

F. Auzel
Centre National d'Etudes des Télécommunications, 196 rue de Paris, 92220 Bagneux, France
(Received 23 September 1975)

Experimental demonstration of multiphonon-assisted anti-Stokes and Stokes excitation of rare-earth ions (R^{3+}) in different hosts, that is, in a weak-coupling ion-lattice interaction case, is obtained. An exponential behavior of excitation probabilities with respect to energy difference between excitation and electronic line is found, just as for multiphonon-assisted nonradiative decay and energy transfer. Exponential parameters α_{AS} and α_S for anti-Stokes and Stokes excitation are measured and linked to the Miyakawa-Dexter α parameter for decay, leading to estimates for Pekar-Huang-Rhys coupling parameter S_0 of about 0.04, in agreement with values obtained from one-phonon spectra or nonradiative-decay measurements. A semiempirical formula is deduced to obtain α from only one parameter, an effective phonon energy.

I. INTRODUCTION

Until now, works devoted to multiphonon-assisted phenomena correlated with triply ionized rare-earth fluorescence have primarily considered nonradiative decays and energy transfers[1-3]. Little experimental work has been devoted to multiphonon-assisted anti-Stokes and Stokes sideband excitation in this weak-coupling limit.

Following the classification of Bron and Wagner,[4] four extreme cases may be distinguished for the general problem of electron-lattice coupling:

(a) Small change in mass and spring constants and weak electron-lattice coupling. This, for example, is the case of triply ionized rare earths in rare-earth halide matrices, where there are usually restrictions to one-phonon sidebands.

(b) Small change in mass and spring constants and strong electron-lattice coupling. This is the case, for instance, of some divalent rare earths such as Sm^{2+} in CaF_2 with one-phonon sidebands.

(c) Large change in mass and spring constants, and strong coupling. This is the case of some divalent rare earths, and also of F center in KCl, which shows multiphonon sidebands up to the tenth order.

(d) Large change in mass and spring constants, and weak coupling in which case only limited vibronic line structure has to be expected. This is the case when the doping impurity strongly alters the phonon modes, and there is the possibility for localized modes.

Since triply ionized rare-earth ions (R^{3+}) in usual matrices for laser, or summation of photon action by energy transfer,[5] appear to fall in class (a), it can be easily understood why very little or no experimental work on multiphonon sidebands of R^{3+} can be found in the literature.[6,7] In Ref. 7 there is, to our knowledge, the only previous result of this type: a curve showing Stokes multiphonon excitation for $NdCl_3$ obtained by Gandrud, with no further comments.

Yet Miyakawa and Dexter have assumed by analogy, with divalent rare-earth ions, that multiphonon sidebands are intermediate steps in the theoretical calculation of the overlap integral appearing in multiphonon-assisted energy transfers between R^{3+},[8] which can also be linked to multiphonon nonradiative transitions. So experiments involving multiphonon sidebands of R^{3+} could give some insight into nonradiative transitions, and energy transfers.

By using a cw dye-laser irradiation, we succeeded in exciting R^{3+} levels far beyond either side of their electronic and one-phonon vibronic absorption range.

Figure 1 gives the energy scheme for different multiphonon phenomena: nonradiative decay, energy transfer, multiphonon anti-Stokes and Stokes excitation—the objects of this paper.

The energy gap ΔE involved between the excitation and the electronic level is larger than $\hbar\omega_m$, the highest phonon frequency of the host; this fact and the exponential functional form of the probability for anti-Stokes and Stokes excitation with re-

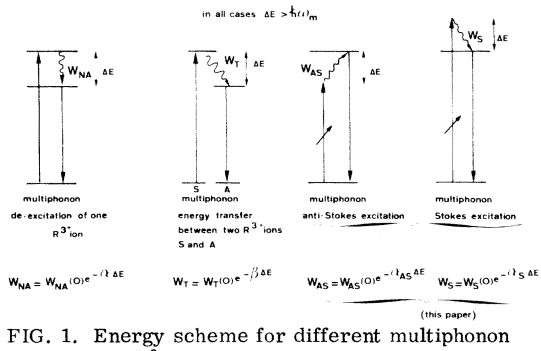

FIG. 1. Energy scheme for different multiphonon phenomena in R^{3+} ions.

spect to an energy gap, similar to those found for decay and transfer, demonstrate that we are dealing with multiphonon phenomena. In the following pages, we are going to discuss the obtainment of these excitations, and their relation to multiphonon decay and transfer through the exponential decay parameters α, β, α_{AS}, and α_S. In this work we do not need to consider absolute values for probabilities, but we consider their functional dependence on ΔE and temperature.

II. EXPERIMENTAL SETUP

The general scheme of the experimental setup is given in Fig. 2. The rhodamine 6G dye laser is a model 370, pumped by a model 164 argon-ion laser, both from Spectra-Physics. The cw output can be tuned from about 0.56 to 0.62 μm, with a maximum energy density of 400 W/cm^2.

The fluorescence of the R^{3+}, which has been conveniently excited, is issued from level $^4S_{3/2}$ of Er^{3+} at 0.54 μm and from $^5F_5$ of Ho^{3+} at 0.65 μm, respectively, for anti-Stokes and Stokes emission. This ion choice was dictated to avoid problems with eventual low-lying levels and to suit the emission range of the dye laser. The R^{3+} fluorescence is carefully separated from excitation scattered light and dye fluorescence by Schott 0G 550 and 0G 570 filters, and two M25 grating monochromators from Jobin-Yvon. Detection of the emission is obtained by an EMI 9558 photomultiplier, the output of which is fed to a preamplifier, a selective amplifier, and a synchronous detector from PAR. The sample is held inside a liquid-nitrogen circulation cryostat, which permits the obtainment of any temperature between 77 and 470 °K. Caution which has to be taken is essentially the same as in a Raman experiment; the difference being that here one-phonon Raman lines are considered as parasitic, and that generally a fixed wavelength is observed and a variable wavelength excitation is used instead of the opposite.

Energy differences are taken between the laser emission and the gravity center of the considered-level Stark group. They are considered significant only when larger than Stark splitting of levels involved in the transition.

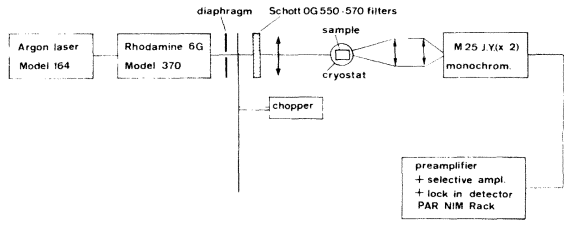

FIG. 2. Experimental setup for multiphonon anti-Stokes and Stokes fluorescence excitation.

Several matrices (CdF_2, WO_4Ca, LaF_3, HoF_3) doped either with Er^{3+} or Ho^{3+} have been considered, but emphasis is given to LaF_3, the host which has been one of the most extensively studied for multiphonon-nonradiative decay[1,2]. This shall give more significance when compared with our results.

To reach the behavior of the multiphonon-excitation probability with respect to temperature, we must also take into account separately the behavior of the emitting level. This was done for $^4S_{3/2}$ Er^{3+} by considering the fluorescence at 0.837 μm of the transition $^4S_{3/2} \rightarrow {}^4I_{13/2}$, when $^4S_{3/2}$ is directly excited in its zero-phonon line. The excitation is then given by a tungsten lamp with filters centered at 0.54 μm, the detection being the same as previously mentioned. To account for the behavior of $^5F_5$ Ho^{3+}, we have measured the $^5F_5$ lifetime with respect to temperature using one-phonon Stokes excitation. The dye-laser emission, concentrated by a microscope objective, is modulated at 200 Hz by a rotating disk with two holes, before impinging onto the crystal. The fluorescence decay is analyzed by a sampling technique.

III. EXPERIMENTAL RESULTS

A. Anti-Stokes excitation

This is the case when the emission from $^4S_{3/2}$ Er^{3+} is obtained at higher energy than its excitation, the energy difference being provided by the annihilation of simultaneous phonons from the lattice at the temperature of the experiment. By verifying that at fixed ΔE emission is linear with excitation intensity, the possibility for multiphoton excitation is eliminated.

Figure 3 exhibits an example of anti-Stokes spectra obtained at room temperature for LaF_3 doped with 1% molar Er per La. To our knowledge, this is the first reported case of multiphonon anti-Stokes excitation in the weak-coupling limit.

Figure 4 exhibits the functional dependence for this anti-Stokes excitation with respect to ΔE, the energy mismatch. It shows that an exponential dependence fits the experimental points quite well at room temperature, as well as at 450 °K.

Figure 5 exhibits the same results obtained for WO_4Ca doped with 2% molar Er per Ca. It shows two bands which are, in fact, two anti-Stokes Raman lines of the host, detected when their separation from excitation equals the ΔE involved. It shows, in this case, that the order of magnitude for a multiphonon anti-Stokes excitation is somewhat less than for the one-phonon anti-Stokes Raman line at 900 cm^{-1}, one of the frequencies of the

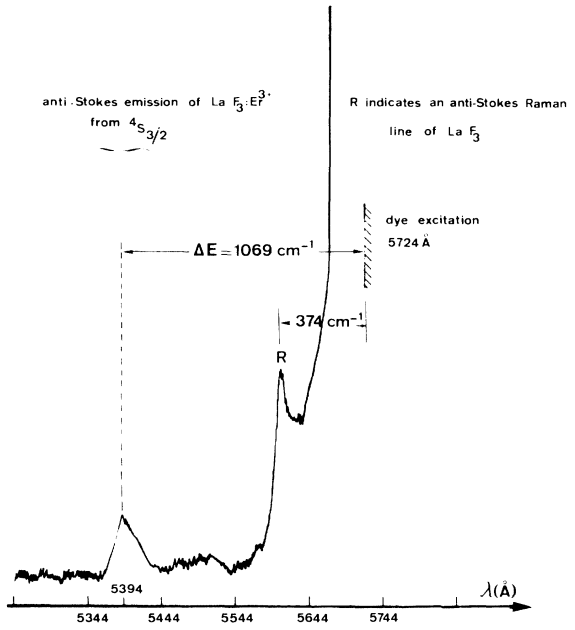

FIG. 3. Anti-Stokes emission at 300 °K of $^4S_{3/2}$ Er^{3+} in LaF_3 excited with an energy mismatch $\Delta E = 1069\ cm^{-1}$.

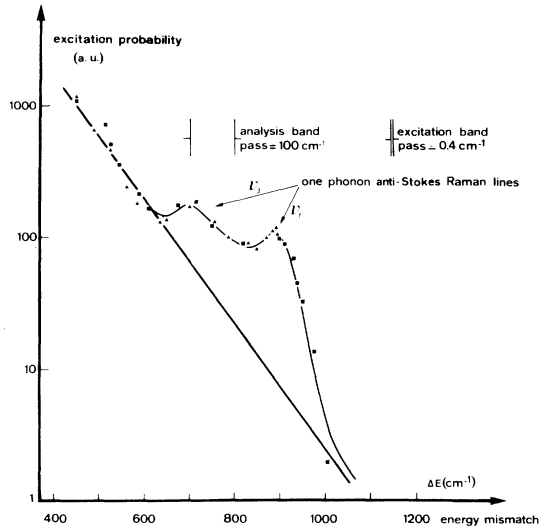

FIG. 5. Functional dependence of multiphonon anti-Stokes excitation with respect to energy mismatch in $WO_4Ca:Er^{3+}$ ($^4S_{3/2}$) at 300 °K.

WO_4^{-2} anion.

An interesting point is that besides the Raman parasitic lines resolved at the low-bandwidth resolution of the double monochromator (>100 cm^{-1}), the multiphonon excitation is resolved at the bandwidth of the exciting laser (≃0.4 cm^{-1}). Even at 77° K there is no spectral structure for the multiphonon excitation, although when the electron-lattice coupling is weak such structure could be expected.[8]

Figure 6 exhibits the spectra for three different excitation energies, showing how anti-Stokes Ra-

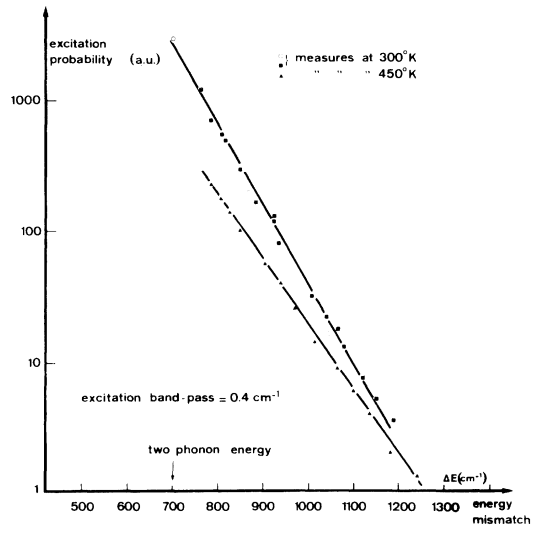

FIG. 4. Functional dependence with respect to energy mismatch ΔE for multiphonon anti-Stokes excitation of $LaF_3:Er^{3+}$($^4S_{3/2}$) at 300 and 450 °K.

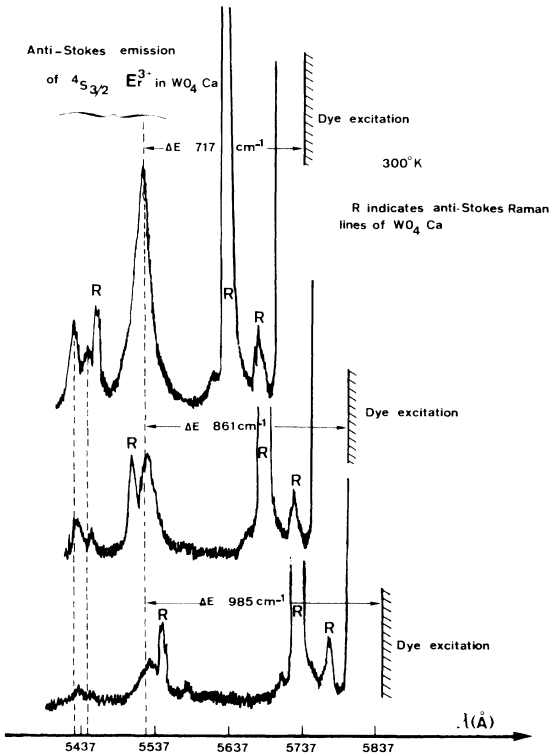

FIG. 6. Anti-Stokes excitation of $^4S_{3/2}$ Er^{3+} for different excitation mismatches.

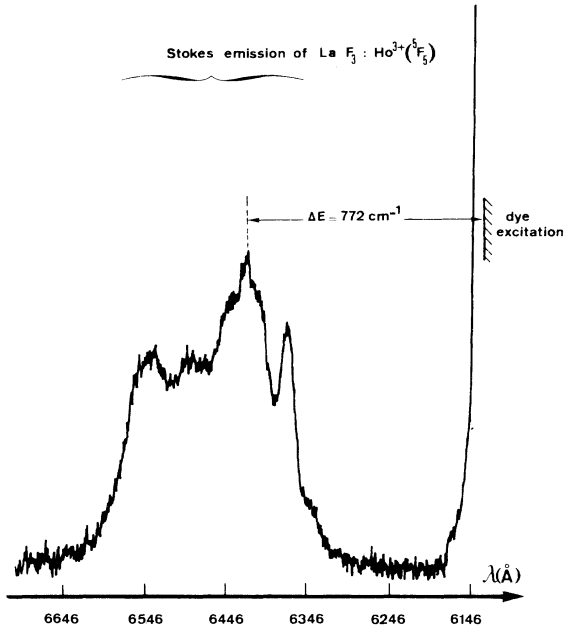

FIG. 7. Stokes emission at 300 °K of LaF_3:Ho^{3+}($^5F_5$) at $\Delta E = 772\ cm^{-1}$.

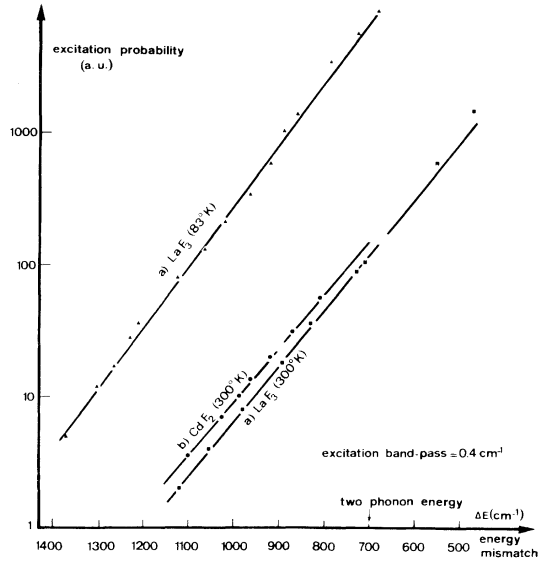

FIG. 8. Functional dependence with respect to energy mismatch for multiphonon Stokes excitation of (a) LaF_3: Ho^{3+}($^5F_5$) at 300 °K and 83 °K and (b) CdF_2:Ho^{3+}($^5F_5$) at 300 °K.

man lines may interfer with anti-Stokes fluorescence when ΔE corresponds to a Raman line. Both types of lines may be easily distinguished by the fact that Raman lines stay at fixed relative energy from the excitation laser energy, whereas the fluorescence lines stay at fixed absolute energy. This shows that multiphonon excitation is still possible at ΔE smaller than the 900 cm^{-1} one-phonon Raman line and gives an indication that for matrices with a phonon gap in the phonons spectra, such as WO_4Ca, the effective energy phonons are at lower energy than the highest mode of WO_4^{-2}.

B. Stokes excitation

In this case, owing to the limited tuning range of our dye laser, we have chosen another ion's level, assuming, as has been generally found for nonradiative decay, that there are no strong symmetry selection rules in the multiphonon ion-lattice coupling. Here, $^5F_5$ Ho^{3+} emitting at 0.65 μm is considered. The energy difference with excitation is given to the lattice by creation of simultaneous phonons.

Figure 7 gives an example of Stokes spectra obtained for LaF_3:Ho^{3+}. Figure 8 presents the dependence of the relative excitation probability with respect to energy mismatch ΔE. Here again, an exponential decrease is found for (a) LaF_3:Ho^{3+}, (b) CdF_2:Ho^{3+}.

The temperature behavior of anti-Stokes and Stokes excitation in LaF_3 shall be discussed in Sec. IV in relation to the multiphonon nonradiative decay.

IV. DISCUSSION AND CORRELATION WITH NONRADIATIVE-DECAY PARAMETERS AND MULTIPHONON-ASSISTED ENERGY TRANSFER

A. Miyakawa-Dexter theory and multiphonon excitation

Using the Kubo-Toyozawa-Lax generating-function method, adiabatic approximation, and linear coupling, Miyakawa and Dexter[8] have shown that a common theoretical treatment is possible for the three following multiphonon processes: side-bands absorption $A(\nu)$, relaxation rate W_{NA} due to the Hamiltonian's small nonadiabaticity, and phonon-assisted energy-transfer probability from ion a to ion b, W_{ab}.

In the case of small-g coupling constant (low temperature with respect to maximum phonon energy of the lattice), Miyakawa and Dexter have obtained the following expressions:

$$A(\nu) = (8\pi^3 N_a/3hc)\nu |M|^2 \sum_{m=0}^{\infty} \frac{e^{-g} g^m}{m!} \delta(h\nu - m\hbar\omega) \quad (\text{at } T = 0^\circ\text{K}), \tag{1}$$

$$W_{NA} = (2\pi/\hbar)[g^N(\bar{n}+1)^N/N!]R^2(1-N/g)^2\delta(\epsilon_0 - N\hbar\omega) \quad (\text{at } T < \hbar\omega_m/k), \tag{2}$$

$$W_{ab} = (2\pi/\hbar)\,|H_{ab}|^2 \sum_N e^{-(g_a+g_b)}(g_a+g_b)^N/N!\,\sigma_{ab}\delta(\epsilon_0 - N\hbar\omega) \quad (\text{at } T = 0^\circ\text{K}), \tag{3}$$

where N_a is the number of absorbing ions; $|M|$ is the matrix element for optical absorption; g is the electron-phonon coupling function related to S_0, the Pekar-Huang-Rhys coupling constant, by $g = S_0(2\bar{n}+1)$, $\bar{n}$ being the occupation number for the effective phonons of energy $\hbar\omega_m$ where ω_m is assumed to be the maximum lattice frequency; R is the nonadiabatic coupling function; N or m is the order of the multiphonon process involved; σ_{ab} is the overlap integral between ions a and b for zero-order process; $|H_{ab}|$ is the matrix element for interaction between a and b; and $\epsilon_0 \equiv \Delta E$, the energy difference spanned by the multiphonon process.

In each case, Stirling's approximation for $N!$ $[N! \simeq (N/e)^N]$ leads to an approximate exponential functional dependence with respect to the multiphonon order process taken as $N = \Delta E/\hbar\omega_m$.

These dependences for Eqs. (2) and (3) have been given in Ref. 8 to be

$$W_{NA}(\epsilon_0) \simeq (2\pi/\hbar)R^2(1-N/g)^2 e^{-\alpha\epsilon_0}, \tag{2'}$$

with

$$\alpha = (\hbar\omega)^{-1}\{\ln[\bar{N}/g(\bar{n}+1)] - 1\}, \tag{4}$$

and

$$W_{ab}(\epsilon_0) \simeq (2\pi/h)\,|H_{ab}|^2\sigma_{ab}e^{-(g_a+g_b)}e^{-\beta\epsilon_0}, \tag{3'}$$

with

$$\beta = \alpha - (\hbar\omega)^{-1}\ln(1+g_b/g_a), \tag{5}$$

$\bar{N}$ being the average number of phonons involved.

In order to compare sideband absorptions, multiphonon excitation, nonradiative decay, and energy transfer, we put Eq. (1) into exponential form. Since we are interested in absorption probability, (1) is transformed as

$$W(\nu) = (I/c)(8\pi^3/3h^2)\,|M|^2 \times \sum_{m=0}^{\infty}(e^{-g}g^m/m!)\delta(h\nu - m\hbar\omega),$$

where I is the incoming light intensity at frequency ν. Each term $e^{-g}g^m/m!$ in the summation is known to be the integrated shape function for a m-phonon process[9]; our interest being not in the total absorption probability but in the way it is distributed in a function of m, and assuming that only one phonon frequency $\hbar\omega_m$ is effective for each ΔE $(= N\hbar\omega_m)$ considered, we have partial probabilities for each N:

$$W(N) = [I(N)/c](8\pi^3/3h^2)\,|M|^2 e^{-g}g^N/N!, \tag{6}$$

which can also be written with Stirling's approximation.

At this point we must discuss what is happening at room temperature in order to make comparisons with experiments at this temperature.

B. Variation of nonradiative decay and multiphonon absorption with temperature

Riseberg and Moos[2] have found that the experimental variation of W_{NA} is well described up to 400°K by

$$W_{NA}(T) = W_{NA}(0)(\bar{n}+1)^N. \tag{7}$$

Then Eqs. (7) and (2′) can be compatible only if $g = S_0$. There is some ambiguity in Ref. 8, since the same g is considered at $T = 0$°K and at low temperatures. Then, since $\bar{n} \ll 1$, the absolute difference is negligible, but the way the probability changes with temperature is quite different from Eq. (7):

$$W_{NA}(T) = W_{NA}(0)(2\bar{n}^2 + 2n + 1)^N,$$

which cannot account for the experiments of Ref. 2 when temperature is higher than about 150°K. For this reason, in the following we take $g \equiv S_0$ and associate the same variation with temperature as the one proposed for decay in Refs. 10 and 11, with any "Pekarian" forms at 0°K $(e^{-S_0}S_0^N/n!)$ in the three processes in which phonons are emitted, that is

$$e^{-S_0}S_0^N/N!\,F_N(T, S_0),$$

with

$$F_N(T, S_0) = e^{-2S_0\bar{n}}\sum_{l=0}^{\infty}\frac{N!}{l!\,(l+N)!}(1+\bar{n})^{l+N}(\bar{n}S_0^2)^l. \tag{8}$$

For small $\bar{n}$, S_0 and large N, Eq. (8) reduces to $(\bar{n}+1)^N$, the same variation as in Eq. (7).

The summation in Eq. (8) is a converging series, and if one considers only the first term $(l = 0)$ $e^{-2S_0\bar{n}}(1+\bar{n})^N$, one finds the variation with temperature proposed by Fong *et al.*,[12] which also has been shown to describe well experimental results for nonradiative transition. The correspondence in their notation being $S_0 \equiv \frac{1}{4}L_m g_m^2$, L_m being an effective degeneracy factor. In fact, with small values for S_0, $e^{-2S_0\bar{n}}$ can be considered in this first study as a correction we shall neglect (maximum value $\simeq 4\%$ for LaF_3).

As a result, at temperature T we shall consider the function $e^{-S_0}S_0^N/N!\,(1+\bar{n})^N$ giving the correct variation with temperature for nonradiative decay and which we shall use for multiphonon Stokes excitation as well, assuming that phonons are mainly emitted:

$$W_{\text{Stokes}}(N) = \frac{I(N)}{c}\,\frac{8\pi^3}{3h^2}\,|M|^2\,\frac{e^{-S_0}S_0^N}{N!}\,(1+\bar{n})^N. \tag{9}$$

For anti-Stokes excitation, where phonons are mainly absorbed, we have equivalently

$$W_{\text{anti-Stokes}}(N) = \frac{I(N)}{c}\,\frac{8\pi^3}{3h^2}\,|M|^2\,\frac{e^{-S_0}S_0^N}{N!}\,(\bar{n})^N. \tag{10}$$

The variation with temperature is included in $\bar{n} = (e^{-\hbar\omega_m/kT} - 1)^{-1}$.

By using Stirling's developments, Eqs. (9) and (10) are written

$$W_{\text{Stokes}}(\Delta E) = \frac{I}{c}\,\frac{8\pi^3}{3h^2}\,|M|^2 e^{-S_0} e^{-\alpha S^{\Delta E}}, \tag{9'}$$

$$W_{\text{anti-Stokes}}(\Delta E) = \frac{I}{c}\,\frac{8\pi^3}{3h^2}\,|M|^2 e^{-S_0} e^{-(\alpha_S + 1/kT)\Delta E}, \tag{10'}$$

with α_S defined as in Eq. (4), but with $g \equiv S_0$.

$$\alpha_S = (\hbar\omega_m)^{-1}\{\ln[N/S_0(\bar{n}+1)] - 1\} \tag{11}$$

In Eqs. (9′) and (10′), $N! \simeq (N/e)^N$ has been used as in Miyakawa and Dexter instead of the more precise $N! \simeq (2\pi N)^{1/2}(N^2/e)^N$. For low values of N, the slow variation of $N^{1/2}$ does not essentially change the functional behavior, and we shall use the same approximation as in Ref. 8.

From Eqs. (9′) and (2′), identical approximate exponential behavior should be found for nonradiative decay and multiphonon Stokes excitation. In fact, as shown in Table I, all experimental α_S for excitation are larger than the α for nonradiative decay in a systematic way. This discrepancy arises, in our view, from the fact that Eq. (9′) is less approximate than (2′); the factor $(1 - N/g)^2$ should be taken into account by modifying slightly the definition of α. Since $g \ll N$ (weak-coupling multiphonon process), we approximate this factor as N^2/g^2 and include it in the exponential parameter as

$$\alpha_{\text{nonradiative}} = (\hbar\omega_m)^{-1}[(1 - 2/\bar{N})\ln(\bar{N}/S_0) - 1 - \ln(\bar{n}+1)],$$

which is the new relation we propose instead of Eq. (4).

In summary we have:

$$\alpha_{\text{nonradiative}} = \alpha_S - (\hbar\omega_m)^{-1}(2/\bar{N})\ln(\bar{N}/S_0),$$

$$\beta_{\text{transfer}} = \alpha - (\hbar\omega_m)^{-1}\ln 2,$$

$$\alpha_S = (\hbar\omega_m)^{-1}\{\ln[\bar{N}/S_0(\bar{n}+1)] - 1\},$$

$$\alpha_{AS} = \alpha_S + 1/kT.$$

By measuring α_S or α_{AS} by the method of this paper, one can reach α or β, provided S_0, $\bar{N}$, and $\hbar\omega_m$ are known. Conversely, by comparing experimental results for α and α_S, we obtain $\bar{N}$ and S_0. Values obtained by this method in Table I are in accordance with results from literature as obtained by other means.

C. Relation between multiphonon-excitation probability and multiphonon-excited fluorescence intensity

In the described experiment, one obtains fluorescence intensity with respect to excitation energy assuming that thermal equilibrium is reached before emission (no hot luminescence). It is simply proportional to excitation probability that we are interested in. When temperature is varied, the efficiency of the electronic transition has to be taken into account.

At equilibrium, when there are as many excited ions by a multiphonon process as decaying ions by a radiative and nonradiative process, we have

$$W(\Delta E)N_0 = N_1(A + W_{NA}),$$

where $W(\Delta E)$ is the multiphonon excitation probability as given by (9′) or (10′); A is the spontaneous emission probability; N_0 is the ion concentration; and N_1 is the number of ions in the excited level under consideration.

I_f being the related fluorescence intensity,

$$I_f = N_1 A h\nu_f,$$

therefore,

$$W(\Delta E)N_0 = \frac{I_f}{h\nu_f}\,\frac{A + W_{NA}}{A} = \frac{I_f}{h\nu_f}\,\frac{\tau_0}{\tau} = \frac{I_f}{h\nu_f \eta}.$$

τ_0 is the radiative lifetime and τ is the measured lifetime of the considered level, η is the quantum efficiency, and I_f is proportional to the product $\tau W(\Delta E)$. As long as τ or η is constant, I_f has the same functional dependence as $W(\Delta E)$, but this is usually not the case when temperature is varied.

Besides the anti-Stokes excitation of $^4S_{3/2}$ Er^{3+}, we have monitored the dependency of η with temperature by considering the variation of the 0.837-μm emission from the $^4S_{3/2} - {}^4I_{13/2}$ transition with respect to temperature for direct excitation in the $^4S_{3/2}$ electronic line. This variation is deducted from anti-Stokes emission to obtain the variation with temperature for anti-Stokes excita-

TABLE I. Comparison between α_S (this work) and α (literature) and deduced values for the lattice-ion coupling parameter $g(=S_0)$.

Host	$\hbar\omega_m$ (cm^{-1}) from literature	α_S (10^{-3} cm) measured at 300 °K	α (10^{-3} cm) [a] (at 300 °K) from literature	$g(=S_0)$ obtained from comparison with α_S and α	g from literature	$\langle\Delta E\rangle$ (cm^{-1}) ($\bar{N}$)	Comments
$LaBr_3$	175 (Ref. 2)		16		0.04 [d]		
$NdCl_3$	≃255 [b]	16.7	11.4 assumed same as $LaCl_3$	0.03		2110 (8.2)	α_S extracted from an experimental result of Gandrud given in Ref. 7
$LaCl_3$	260 (Ref. 2)		11.4		0.04 [d] 0.05 [d]		
HoF_3	≃320 [b]	12	5 assumed same as LaF_3	0.03		1600 (5)	α_S from Stokes excitation of Ho^{3+} $^5F_5$ compared with α for LaF_3
CdF_2	≃320 [b]	9.5					α_S from Stokes excitation of Ho^{3+} $^5F_5$
LaF_3	350 (Ref. 2)	9.4 8.9 9.7 10	5	0.05	0.02 [c] 0.04 [d]	1890 (5.4)	α_S obtained from anti-Stokes excitation of Er^{3+} $^4S_{3/2}$ at 300 and 450 °K α_S obtained from Stokes excitation of Ho^{3+} $^5F_5$ at 300 °K α_S obtained from Stokes excitation at 80 °K and corrected at 300 °K by Eq. (7)
SrF_2	360 (Ref. 2)		3.9				
WO_4Ca	400 900 (Ref. 15)	6					α_S from anti-Stokes excitation of Er^{3+} $^4S_{3/2}$
Y_2O_3	550 (Ref. 2) 430 (Ref. 16)		3				

[a] Calculated at 300 °K using Eq. (7) and experimental results at 4.2 °K from Ref. 2.
[b] Extrapolated from results with LaF_3, SrF_2, $LaCl_3$, respectively.
[c] Measured for YF_3 by comparing one-phonon and zero-phonon transitions (Ref. 14).
[d] Calculated from nonradiative-decay fittings (Ref. 12).

tion probability alone.

Figure 9 gives the experimental points obtained for $W_{\text{anti-Stokes}}(T)$, and shows that a good fit is given by the combination of Eqs. (10′) and (11), whose temperature-depending part is

$$\exp\left[-\Delta E\left[\left(\frac{1}{kT}-\frac{\ln(\bar{n}+1)}{\hbar\omega_m}\right)\right]\right].$$

As for Stokes excitation of $^5F_5$ Ho^{3+}, we have measured the $^5F_5$ lifetime with respect to temperature when excitation is made at about one phonon distance above $^5F_5$, assuming the one-phonon process is much shorter than the shortest lifetime at any considered temperature. Again, lifetime variations are deducted to reach Stokes excitation probability alone.

Figure 10 gives the results obtained for Stokes excitation probability $W_{\text{Stokes}}(T)$ for $\Delta E = 1500\ \text{cm}^{-1}$; it shows that the corresponding temperature-dependent part Eqs. (9′)–(11), $e^{\Delta E[\ln(\bar{n}+1)/\hbar\omega_m]}$, gives a good fit for $\bar{N}=4$ and $\hbar\omega_m = 374\ \text{cm}^{-1}$, which is slightly higher than the effective frequency usually assumed, but which corresponds to the Raman line found in Fig. 3.

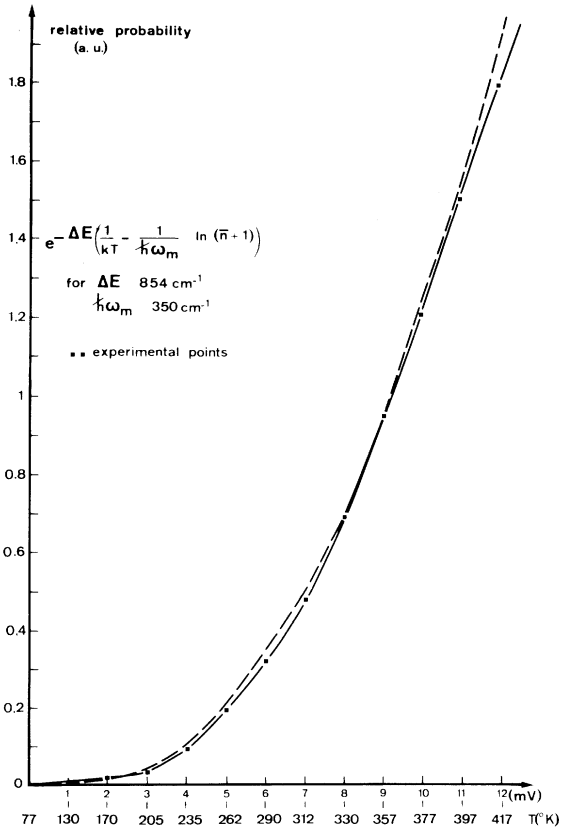

FIG. 9. Relative anti-Stokes excitation probability with respect to temperature of $LaF_3:Er^{3+}(^4S_{3/2})$ for $\Delta E = 854\ \text{cm}^{-1}$ as corrected for $^4S_{3/2}$ efficiency variation through 0.84-μm emission intensity.

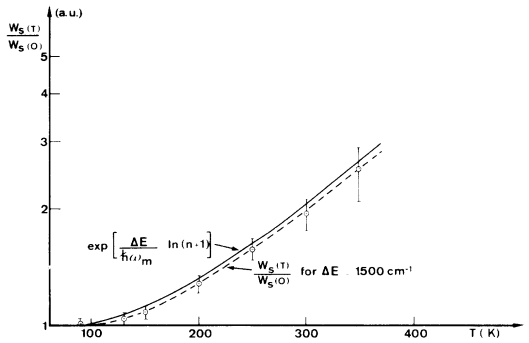

FIG. 10. Relative Stokes excitation probability with respect to temperature of HoF_3 ($^5F_5$) for $\Delta E = 1500\ \text{cm}^{-1}$ as corrected for $^5F_5$ efficiency variations through $^5F_5$ lifetime variations.

Comparison of the results presented in Table I shows that, as explained previously, α_S is always found to be larger than α, but that its classification according to $\hbar\omega_m$ is the same. On the other hand, it can be seen that $\langle\Delta E\rangle = \hbar\omega_m\bar{N}$ and $g(\equiv S_0)$ do not vary much from one matrix to the other, being, respectively, about 2000 cm^{-1} and 0.04 as average.

For practical purposes, it is then possible to give a simplified expression for α (or β) with respect to $\hbar\omega_m$, only. That is, Eqs. (12) and (13) with $\bar{g}(=S_0)=0.04$, and $\bar{N}=2000/\hbar\omega_m$ (for $\hbar\omega_m \leq 650\ \text{cm}^{-1}$). If $\hbar\omega_m$ for Y_2O_3 is taken to be 430 cm^{-1}, instead of 500 cm^{-1},[16] a better fit is obtained for $\langle\Delta E\rangle = 1674\ \text{cm}^{-1}$ and $\bar{g}(=S_0)=0.032$, since α is not very sensitive to $\langle\Delta E\rangle$ or $\bar{g}$ when $\hbar\omega_m$ is not well defined.

Such a simplified formula could be used in predicting optimized matrix for yielding an up-conversion effect.[13]

Figure 11 shows experimental values for α and

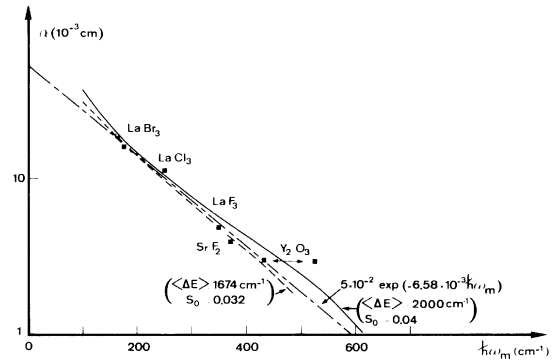

FIG. 11. Fitting curves for

$$\alpha(\hbar\omega_m) = \hbar\omega_m^{-1}\left(\ln\frac{\langle\Delta E\rangle}{\hbar\omega_m S_0(n+1)} - 1 - \frac{2\hbar\omega_m}{\Delta E}\ln\frac{\langle\Delta E\rangle}{\hbar\omega_m S_0}\right).$$

values given by simplified formula. In fact as shown on this figure, a simpler experimental relation could also be used:

$$\alpha(\hbar\omega_m) = 5\times 10^{-2} \exp(-6.5\times 10^{-3}\hbar\omega_m),$$

in the range $175 < \hbar\omega_m < 500$ cm^{-1}, α being in cm and $\hbar\omega_m$ in cm^{-1}.

This results show that, at least in the considered matrices, $\hbar\omega_m$ is the most important parameter with respect to energy mismatch for multiphonon phenomena in R^{3+} ions and can roughly describe nonradiative decay, energy transfer, and excitation.

V. CONCLUSION

We have demonstrated that anti-Stokes or Stokes excitation of R^{3+} ions is possible through multiphonon interaction, that is, in a weak-coupling case. We have shown that such experiments lead to an easy new method of studying nonradiative decay and energy-transfer parameters, since energy variation can be tuned at will, instead of being fixed by nature.

So besides their intrinsic interest, the multiphonon-assisted anti-Stokes or Stokes excitations, by dealing with only one ion's level, could be a more precise way to study the role of selection rules in multiphonon interactions, if any, than the direct method using different levels of several ions in a given matrix.

A new expression is given for α (and β), as well as a link with α_S and α_{AS}, this yielding a way to reach g $(=S_0)$.

Finally, in rough estimation for practical purposes, i.e., up conversion or laser effects, two experimental relations for $\alpha(\hbar\omega_m)$ are given, showing that multiphonon phenomena in R^{3+} ions are mainly characterized as regards energy mismatch, for the considered hosts, by one parameter, an effective phonon frequency.

ACKNOWLEDGMENTS

The author wishes to acknowledge the expert technical assistance of D. Meichenin and also to thank G. Grimouille for growing the WO_4Ca crystal, Dr. L. Esterowitz for kindly providing us with the LaF_3 and CdF_2 samples, and Professor T. Miyakawa for an interesting discussion about thermal equilibrium before luminescence emission.

[1]M. J. Weber, Phys. Rev. 157, 262 (1967).
[2]L. A. Riseberg and H. W. Moos, Phys. Rev. 174, 429 (1968).
[3]N. Yamada, S. Shionoya, and T. Kushida, J. Phys. Soc. Jpn. 32, 1577 (1972).
[4]W. E. Bron and W. Wagner, Phys. Rev. 139, A233 (1965).
[5]F. E. Auzel, Proceedings IEEE 61, 758 (1973).
[6]W. M. Yen, W. C. Scott, and A. L. Schawlow, Phys. Rev. 136, A271 (1964).
[7]E. Cohen and H. W. Moos, Phys. Rev. 161, 258 (1967).
[8]T. Miyakawa and D. L. Dexter, Phys. Rev. B 1, 2961 (1970).
[9]M. H. L. Pryce, in *Phonons*, edited by R. W. H. Stevenson (Oliver and Boyd, London, 1966), p. 422.
[10]K. K. Rebane, *Impurity Spectra of Solids* (Plenum, New York, 1970), p. 76.
[11]M. D. Sturge, Phys. Rev. B 8, 6 (1973).
[12]F. K. Fong, S. L. Naberhuis, and M. M. Miller, J. Chem. Phys. 56, 4020 (1972).
[13]F. Auzel and D. Pecile (unpublished).
[14]H. Kuroda, S. Shionoya, and T. Kushida, J. Phys. Soc. Jpn. 33, 125 (1972).
[15]N. Yamada and S. Shionoya, J. Phys. Soc. Jpn. 31, 841 (1971).
[16]N. Yamada, S. Shionoya, and T. Kushida, J. Phys. Soc. Jpn. 32, 1577 (1972).